American Journal of Engineering Research (AJER)
e-ISSN: 2320-0847 p-ISSN : 2320-0936
Volume-12, Issue-4, pp-25-32
www.ajer.org
Research Paper Open Access

Digital Method Of Detection Of A Target With A Multiple Input Multiple Output (Mimo) Radar In The International Airport Of Ndjili In Kinshasa.

Mpole Boyokame Josephine [1], Lidinga Mobonda Flory [2], Meni Babakidi Narcisse [3], Dondo Mebukila François [4], Cimbela Kasongo JG [5] and Maguiraga Madiassa[6].

Abstract: *In this paper, we address the probability of target detection from a MIMO radar at Ndjili International Airport . This article consists of analyzing the distance between the target and the radar using the fact that the signal travels a round trip path. If it is considered that the high frequency radar signal is moving at speed c and that the radar echo of the target is measured after a time t_1 , the target is then detected at a distance . The application of the MIMO concept in the radar system enables the construction of a virtual network larger than the network of the traditional system. This large scale of the virtual network makes it possible to considerably increase the performance in terms of detection for the statistical radar and in terms of location for the coherent radar. The latter is favored by a gain linked to the coherence between the signals whereas the statistical MIMO radar is favored by another gain linked to the spatial diversity.*
Keywords: *Numerical method, Target detection, Radar, Multiple Input Multiple Output, International Airport.*

Date of Submission: 01-04-2023 Date of acceptance: 11-04-2023

I. INTRODUCTION

The Multiple Input Multiple Output (MIMO) concept has shown its effectiveness in the field of telecommunications. The MIMO concept makes it possible to send several different signals on different antennas to increase the performance of the transmission system. Its particularity therefore involves the simultaneous use of several antennas, transmitters and receivers. This concept is completely adaptable to the radar system presented above. MIMO radar can be dened simply as a radar with multiple radiations and multiple receiving sites and the information received is processed together. In other words, MIMO radar is just a generalization of the multistatic concept.

By the most general definition, many traditional systems can be considered special cases of MIMO radar. For example, synthetic aperture radar (SAR) can be considered a form of MIMO radar. Similarly, polarimetric radar , i.e. a radar that measures both polarization components for each transmitted polarization, is an example of MIMO radar. In many existing works, MIMO radar antennas emit signals, which may or may not be correlated, assumed to be orthogonal, but this is not a requirement for MIMO radar. However, orthogonality can facilitate processing.

I.2 RADAR SETTINGS

According to the arrangement of the transmission and reception elements, two main configurations of the radar can be distinguished in the literature. These are monostatic radar and bistatic radar . For technological reasons, the first radars were of bistatic configuration , which appeared in 1930, because the integration of the transmitter and the receiver in the same radar was not completely mastered. But thanks to the implementation of duplexers in 1936, monostatic systems were quickly imposed by their lower cost.

I.2.1 Monostatic radar

monostatic radar , the transmitter and receiver share common electronics and antenna. In this monostatic configuration , the sharing of the electronics and the antenna makes it possible to reduce the bulk and the costs

of synchronization between the transmitter and the receiver, which explains why the vast majority of radars are monostatic

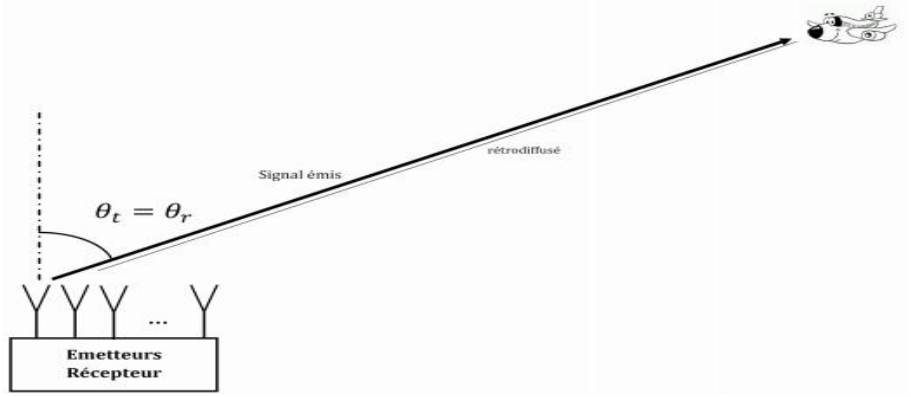

Figure I.1: Monostatic radar configuration

I.2.2 Bistatic radar configuration

bistatic configuration requires good synchronization between the transmitter and the receiver, and the use of a less trivial acquisition geometry. When talking about bistatic radar , it is implicitly assumed that the transmitter and receiver are actually separated (either from a distance point of view or from an angular point of view). If the transmitter and the receiver are physically separate (different antennas) but located almost in the same place, the received signal is qualitatively close to a monostatic signal . One thus speaks of strongly bistatic or weakly bistatic configurations to integrate these two possibilities.

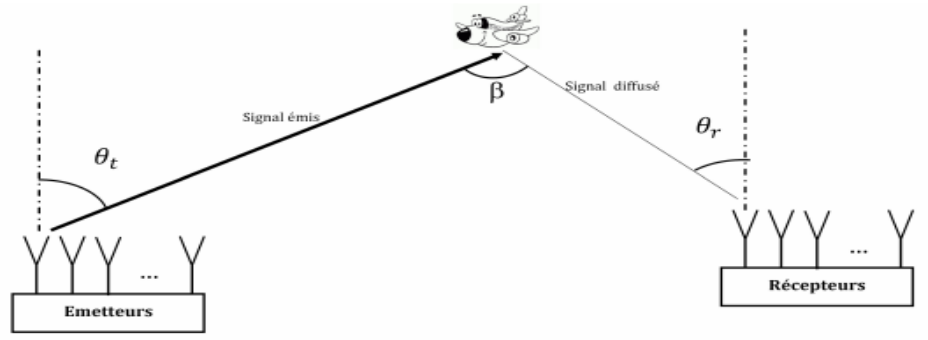

Figure I.2: Configuration of the bistatic radar

I.2.3 Multistatic radar configuration

MIMO radar can be simply defined as a radar with multiple beams and multiple receiving sites and the received information is processed together. In other words, MIMO radar is just a generalization of the multistatic concept.

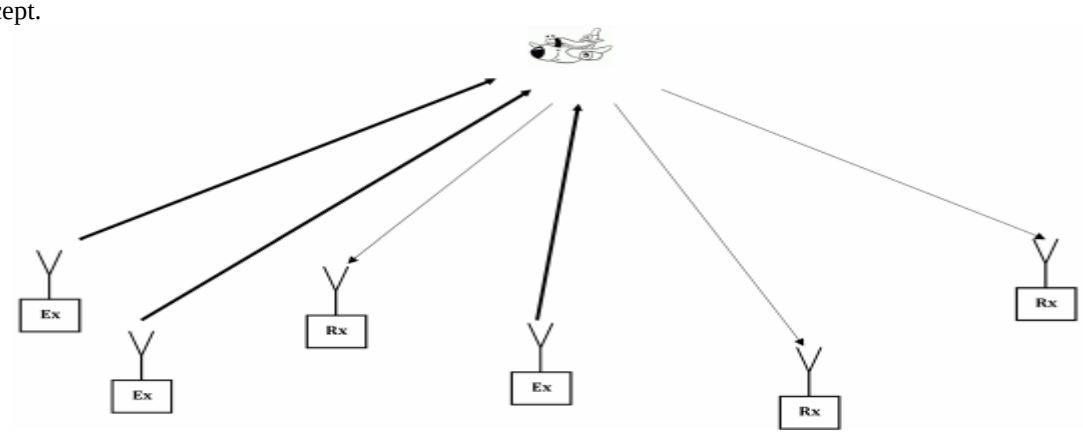

Figure I.3: Configuration of the multistatic radar

I.2.4 Static IMMO Radar signal model

The transmitting antennas are widely spaced (even for the receiving antennas) and therefore the received signals are independent. This MIMO radar is called "the statistical MIMO radar". In this configuration, in which the transmitting elements and the receiving elements are widely spaced, the diversity of the multitude of (spatial) viewing angles increases the performance in terms of detection.

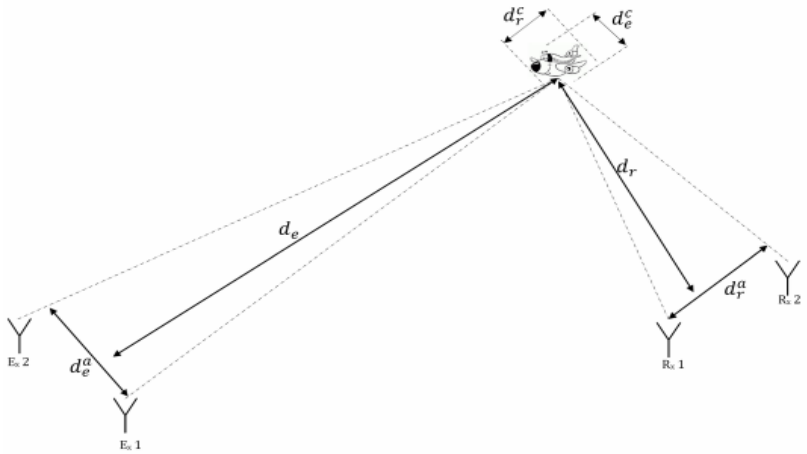

Figure I.2: MIMO Radar

Bistatic MIMO radar signal model

In this configuration, the transmitting elements (as well as the receiving elements) are closely spaced so that the target is in the far field with respect to these arrays, this configuration is called "the coherent MIMO radar". This configuration, where the transmitting and receiving antennas are closely located, is favored by its performance in terms of localization.

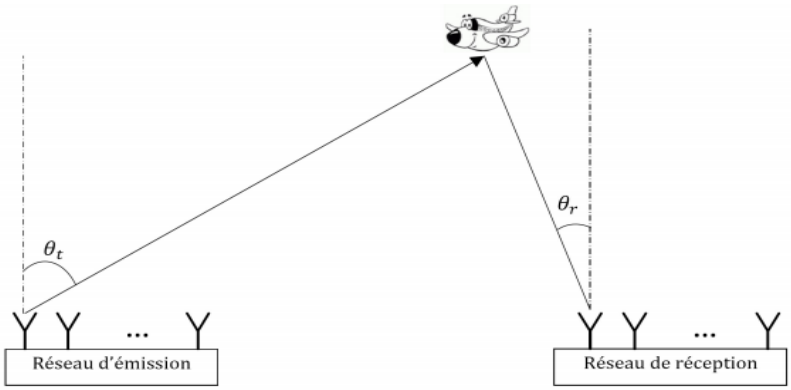

Figure II.3: Bistatic MIMO radar

II. RADAR TARGET LOCATION EQUATIONS

II.1 MIMO Radar Equation

Case 1: Statistical MIMO Radar

$$d_e{}^a > d_e \lambda/_{d_e{}^c} \; et \;\; d_r{}^a > d_r \lambda/_{d_r{}^c} \quad (2.1)$$

Case 2: Coherent MIMO Radar

$$d_e{}^a > d_e \lambda/_{d_e{}^c} \; et \;\; d_r{}^a < d_r \lambda/_{d_r{}^c} \quad (2.2)$$

where λ is the wavelength.

The complex gain, provided by the reflection of the target and which depends on the effective radar surface (SER), is assumed to be a complex random variable. At each pulse, the received signal vector, for a radar system composed of M *transmit and* N antennas receiving antennas, is given by :

$$x(l,t) = \sqrt{\frac{E}{M}} diag\big(a(x_0,y_0)\big) H diag\big(b(x_0,y_0)\big) s(l-\tau,t) + w(l,t) \quad (2.3)$$

For a target located at the azimuthal position (θ_r , θ_t) (where θ_t is the direction relative to the transmission grating called "Departure Direction (DDD)" and θ_r is the direction relative to the transmission grating receiver called "Direction of Arrival (DDA)"), and by exploiting the linear and uniform form of the transmission network and the reception network, the expression (2.4) of the received signal can be rewritten as follows:

$$x(l,t) = \alpha(t) a(\theta_r) b^T(\theta_t) \begin{bmatrix} s_1(l,t) \\ \vdots \\ S_M(l,t) \end{bmatrix} + w(l,t) \qquad (2.4)$$

For better separation of transmitted signals on reception, orthogonal signals are often transmitted i.e. $\big(< s_i(l,t), s_j(l,t) >= 0 \; et \; < s_i(l,t) >= r(t), i \neq j = 1 \ldots M, \big)$where $r(t)$is the baseband signal at the output of the i th matched filter. So, the output of the m th matched filter, corresponds to the waveform emitted by the m th issuer, is given by:

$$y_m(t) = \alpha(t) a(\theta_r) b^T(\theta_t) \begin{bmatrix} 0 \\ \vdots \\ r(t) \\ \vdots \\ 0 \end{bmatrix} + W_m(t) \qquad (2.5)$$

This last expression can be rearranged to obtain the final shape of the signal vector at the reception which corresponds to the waveform emitted by the same transmitter:

$$y_m(t) = \alpha(t) a(\theta_r) b_m(\theta_t) r(t) + w_m(t) \qquad (2.6)$$

II.2 Equation according to the Swerling model

With the transfer matrix given by:

$$C = \big[(\theta_r{}^1, \theta_t{}^1), \ldots., c(\theta_r{}^p, \theta_t{}^p)\big]_{MNxP} \qquad (2.7)$$

$$c(\theta_r{}^1, \theta_t{}^1), \ldots., c(\theta_r{}^p, \theta_t{}^p) \otimes a(\theta_r{}^p) \qquad (2.8)$$

and

$$s(t) = \begin{bmatrix} \alpha_1(t) r_1(t) \\ \vdots \\ \alpha_p(t) r_p(t) \end{bmatrix} \qquad (2.9)$$

Depending on the target fluctuation models considered, two signal model cases arise here. Case of the Swerling I model: the backscattering coefficients are considered constant from one pulse to another and therefore:

$$s(t) = \begin{bmatrix} \alpha_1 r_1(t) \\ \vdots \\ \alpha_p r_p(t) \end{bmatrix} \qquad (2.10)$$

Case of the Swerling II model: the backscattering coefficients change from one pulse to another:

$$s(t) = \begin{bmatrix} \alpha_1(t) r_1(t) \\ \vdots \\ \alpha_p(t) r_p(t) \end{bmatrix} \qquad (2.11)$$

identical baseband signals r (t).

II.3 TARGET EQUATION

II.3.1 Covariance matrix

Most high-resolution antenna processing methods exploit the properties of the covariance matrix of received signals to minimize the influence of noise. The model of the signal considered is that given by the expression:

$$z(t) = Cs(t) + n(t) \qquad (2.12)$$

The targets, assumed to be in the same range box, fluctuate according to the Swerling II model. Therefore, in all cases the elements of the signal vector $s(t)$are not totally correlated. The covariance matrix of the observation vector $z(t)$is given by:

$$R = E[z(t)z^H(t)] \qquad (2.13)$$

Substituting the expression (2.13) of the signal model adopted in the equation above, we obtain:

$$R = CR_{ss}C^H + {\sigma_n}^2 I_{MN} \qquad (2.14)$$

with R_{ss} the covariance matrix of the transmitted signals and${\sigma_n}^2 I_{MN}$ the noise covariance matrix assumed, in this work, zero-mean Gaussian complex. In practice, the covariance matrix is estimated from the temporal samples of the vector of observations:

$$\hat{R} = \frac{1}{T}\sum_{t=1}^{T} z(t)z^H(t) \qquad (2.15)$$

II.3.2 Cramèr - Rao BCR terminal

The BCR has been calculated and discussed in terms of localization , in addition, this Cramèr -Rao limit has also been discussed for the optimization of the waveform in MIMO radar.
The BCR is dened as the inverse of the Fisher Information Matrix (FIM):

$$BCR(\eta) = diag\big(j - 1(\eta)\big) \qquad (2.16)$$

For the case of gure , a coherent bistatic MIMO radar whose signal model is given by (3.23), the MIF can be calculated as follows:

$$J(\eta) = \frac{1}{2}tr\left[R^{-1}(\eta)\frac{\partial R(\eta)}{\partial \eta}R^{-1}(\eta)\frac{\partial R(\eta)}{\partial \eta}\right] = \begin{bmatrix} J_{\theta_{r,}\theta_{r,}} & J_{\theta_{r,}\theta_{t,}} & J_{\theta_{r,}\sigma_\alpha} & J_{\theta_{r,}\sigma} \\ J^T{}_{\theta_{r,}\theta_{r,}} & J_{\theta_{t,}\theta_{t,}} & J_{\theta_{t,}\sigma_\alpha} & J_{\theta_{t,}\sigma} \\ J^T{}_{\theta_{r,}\sigma_{\alpha,}} & J^T{}_{\theta_{t,}\sigma_{\alpha,}} & J_{\theta_{r,}\sigma_\alpha} & J_{\sigma_{\alpha,}\sigma} \\ J^T{}_{\theta_{r,}\sigma} & J^T{}_{\theta_{t,}\sigma} & J^T{}_{\sigma_{\alpha,}\sigma} & J_{\sigma,\sigma} \end{bmatrix} (2.17)$$

The derivatives can be calculated as follows:

$$\frac{\partial R(\eta)}{\partial {\theta_r}^{(p)}} = \frac{1}{2}{\sigma^2}_{\alpha p}\frac{\partial c\big({\theta_r}^{(p)}, {\theta_t}^{(p)}\big)c^H\big({\theta_r}^{(p)}, {\theta_t}^{(p)}\big)}{\partial {\theta_r}^{(p)}} \quad (2.18)$$

$$\frac{\partial R(\eta)}{\partial {\theta_t}^{(p)}} = \frac{1}{2}{\sigma^2}_{\alpha p}\frac{\partial c\big({\theta_r}^{(p)}, {\theta_t}^{(p)}\big)c^H\big({\theta_r}^{(p)}, {\theta_t}^{(p)}\big)}{\partial {\theta_t}^{(p)}} \quad (2.19)$$

$$\frac{\partial R(\eta)}{\partial \sigma_{\alpha p}} = 2\sigma_{\alpha p}\partial c\big({\theta_r}^{(p)}, {\theta_t}^{(p)}\big)c^H\big({\theta_r}^{(p)}, {\theta_t}^{(p)}\big) \quad (2.20)$$

$$\frac{\partial R(\eta)}{\partial \sigma} = 2\sigma I_{MN} \quad (2.21)$$

Therefore, the BCRs relating to the estimation of the DDA are the P first BCR elements (η) and the BCRs relative to the DDD estimate are the P following items.

III. DISCUSSIONS AND SIMULATION ON BCR

III.1 Simulation of the results

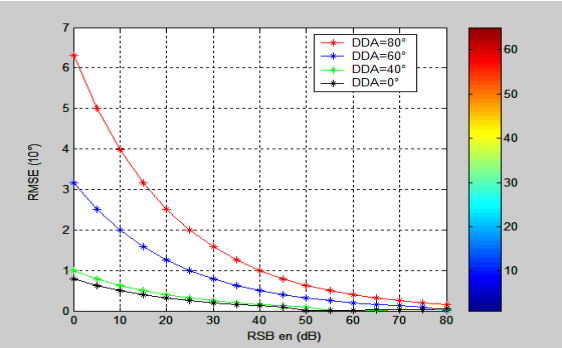

Figure 3.1: Effect of the position of the target

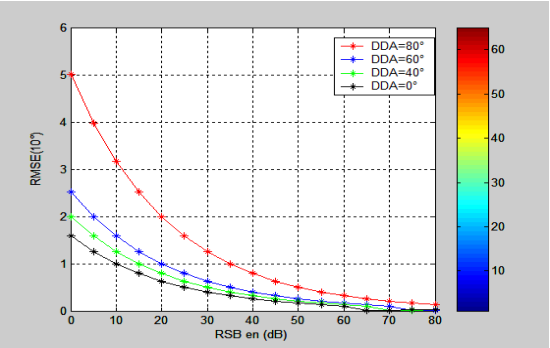

Figure 3.2: Effect of starting angle on estimation error

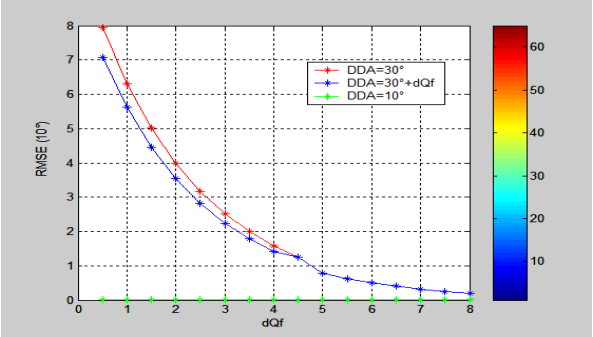

Figure 3.3: Effect of adjacent targets on DDA estimation

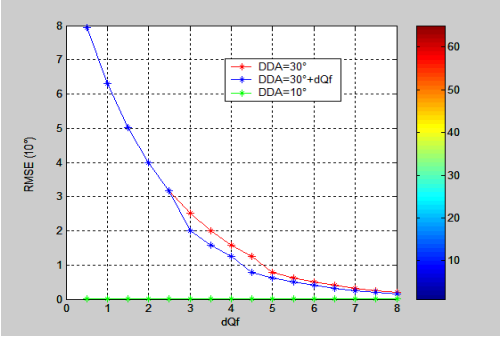

Figure 3.4: Effect of adjacent targets on DDD estimation

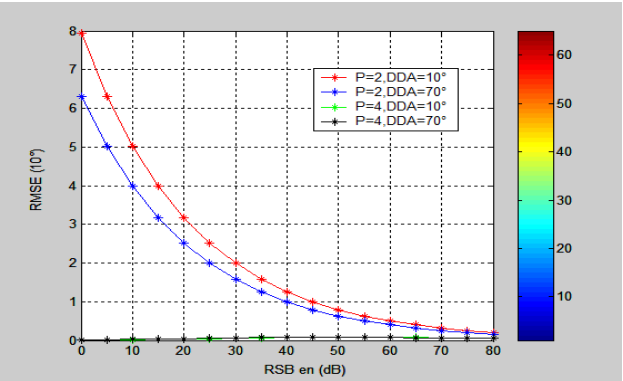

Figure 3.5: Effect of number of targets on the estimation of DDA

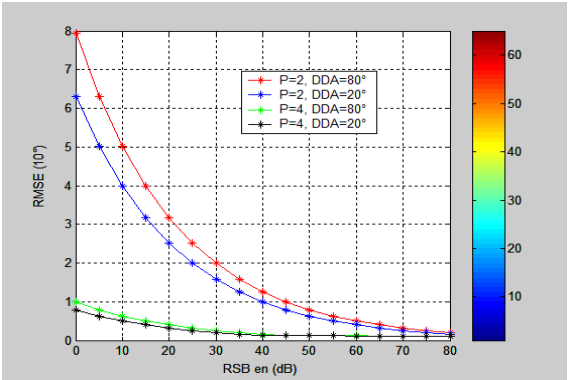

Figure 3.6: Effect of number of targets on DDD estimation

III.2 Interpretation of results

We have just examined in this simulation the behavior of the BCR relative to the direction of the target, the resolution and the number of targets to locate. The bistatic coherent MIMO radar considered consists of two linear and uniform arrays, the first is composed of M = 3 transmitting antennas spaced by half a wavelength and the second of N = 4 receiving antennas also spaced by half a wavelength. -wave length. The number of pulses is fixed at T = 256 and the number of Monte-Carlo iterations at K = 200

P =3 targets are considered in this case, the first is at ($\theta_r^{(1)}$, $\theta_t^{(1)}$)= (30 °, 30 °), the second at ($\theta_r^{(2)}$, $\theta_t^{(2)}$)=(30 ° +Δ θ, 30 ° +Δ θ) and the third is at the position ($\theta_r^{(3)}$, $\theta_t^{(3)}$)=(10 °, 10 °). The signal-to-noise ratio is fixed at RSB = 12 dB .

Figures 3.1 and 3.2 show BCR as a function of signal-to-noise ratio for different target positions. These target positions take the values (θ_r, θ_t) = (0 °, 0 °), (40 °, 40 °), (60 °, 60 °), (80 °, 80 °). It can be observed that the error increases with the distance of the target from zero.
Figures 3.3 and 3.4 show the BCR as a function of $\Delta\theta$ for the estimation of DDA and DDD, respectively. We notice that the error of the estimate is inversely proportional to the difference between the targets and that the estimate of the third target is not affected.
In order to show the effect of the number of targets on the joint estimate of DDADDD, we consider two cases P =2 and P =4. The BCR is plotted for the two targets which have the same positions in both cases (i.e. the first target and the second target). The four targets are in the directions: ($\theta_r^{(1)}, \theta t^{(1)}$)=(10 °, 80 °); ($\theta r_{\_}^{(2)}, \theta t^{(2)}$)= (70 °, 20 °); ($\theta r_{\_}^{(3)}, \theta t^{(3)}$)= (50 °, 30 °); ($\theta r_{\_}^{(4)}, \theta t^{(4)}$) = (60 °, 40 °); Figures 3.5 and 3.6 show BCR as a function of SNR for the estimation of DDA and DDD of the first two targets, respectively. We notice that the estimation error increases when the number of targets increases.

IV. CONCLUSION

We saw that this article was about locating a target from the multiple output (MIMO) input radar in Ndjili International Airport. Based on the specific equation according to the environment in which it operates, so that the detection seriously degrades depending on the distance, we have analyzed the parameters influencing the radar equation, for this we have analyzed the influence of the variation of the effective radar surface **σ** and the transmission power P_s . The detection methods presented in this article will lead to the comparison of the received signal to a fixed threshold.

However, a fixed threshold produces either an excessive number of false alarms or a low probability of detection as soon as the statistical characteristics of the noise and the clutter change. This remark is the basis for proposing constant false alarm rate (CFAR) detectors.

BIBLIOGRAPHY

[1]. H. Abeida and J.-P. Delmas . MUSIC-like estimation of direction of arrival for noncircular sources. IEEE Transactions on Signal Processing, 54(7): 2678_2690, 2006. (Cited on pages 3 and 57.)
[2]. Y.I Abramovich and G.J Frazer. Theoretical assessment of MIMO radar performance in the presence of discrete and distributed clutter. In Signals, Systems and Computers, 2008 42nd Asilomar Conference on, pages 629_633, 2009. (Cited on page 2.)
[3]. Yuri I. Abramovich , Gordon J. Frazer, and Ben A. Johnson. Iterative adaptive kronecker MIMO radar beamformer : Description and convergence analysis. IEEE Transactions on Signal Processing, 58(7): 3681_3691, 2010. (Cited on pages 2 and 26.)
[4]. Jian Li, Luzhou Xu , Petre Stoica , Keith W. Forsythe, and Daniel W. Bliss. Range compression and waveform optimization for MIMO radar: A Cramèr - Rao bound based study. IEEE Transactions on Signal Processing, 56(1): 218-232, 2008. (Cited on pages 2 and 26.)
[5]. Hamet Bastien , Obriot Nicolas, “signal modeling and foundation of Near- fied Naval MIMO radar for small targets discrimination” Master thesis In mobile communication systems department of electronic systems alborg university, may 2012.
[6]. Jalal Al -Roomym , Akram Abn-Roidam , “ waveformgeneratron ” January 2010.
[7]. EA Marengo and FK Gruber. Subspace-based localization and inverse scattering of multiply scattering point targets. In EURASIP . Journal on Advances in Signal Processing , number 1, pages 109–112, Dec. 2007.
[8]. M. Tanter , J.-L. Thomas, and M. Fink. Time reversal and the inverse filter. In Acoustical Society of America Journal , pages 223–234 vol.108, July 2000.

BIBLIOGRAPHY

Mpole Boyokame Joséphine , diploma from Engineering 1995 ISTA-KIN in DR of Congo, DEA degree 2020, Doctor student of University national pedagogy of Kinshasa-Congo. of Applied Sciences.

Prof. Dr. Ir Flory Lidinga Mobonda , PhD.2016 In Engineering Sciences, Dept. Of Electricity, University of Brazzaville-Congo. Teacher-Researcher at ISTA-Boma

Prof.Dr.Ir Narcisse Meni Babaka , Ph.D. in Microelectronics Engineering Sciences , of University Michoacana of San Nicolas of Hidalgo (UMSNH) Mexico .2017-2021,
Teacher-Researcher at ISTA-Kinshasa

Dodo Mebukila Francois
Assistant teacher at ISTA-Boma. Master Student . in engineering sciences, the computer network engineer.

Prof.Dr. Ordinaire Cimbela Kasongo Is an physic, from the University National Pedagogy of Kinshasa-Congo.
He is presently lecturer at the University National Pedagogy of Kinshasa-Congo. Dept. of Applied Sciences

Prof.Dr.Ir Maguiraga Madiassa
PhD in Applied Sciences Electronic Engineering.
Teacher-Researcher at UNIKIN